IJNAOE
©SNAK,2015

Int. J. Nav. Archit. Ocean Eng. (2015) 7:466~477
http://dx.doi.org/10.1515/ijnaoe-2015-0033
pISSN: 2092-6782, eISSN: 2092-6790

A numerical study on manoeuvrability of wind turbine installation vessel using OpenFOAM

Sungwook Lee and Booki Kim

Samsung Ship Model Basin, Samsung Heavy Industries Co., Ltd, Daejeon, Korea

Received 1 September 2014; Revised 8 January 2015; Accepted 10 February 2015

ABSTRACT: *In this study, a numerical prediction method on manoeuvrability of Wind Turbine Installation Vessel (WTIV) is presented. Planar Motion Mechanism (PMM) captive test for the bare hull of WTIV is carried out in the model basin and compared with the numerical results using RANS simulation based on Open-source Field Operation And Manipulation (OpenFOAM) calculation to validate the developed method. The manoeuvrability of WTIV with skeg and/or without skeg is investigated using the numerical approach along with the captive model test. In the numerical calculations, the dynamic stability index which indicates the course keeping ability is evaluated and compared for three different hull configurations i.e. bare hull and other two hulls with center skeg and twin skeg. This paper proves that the numerical approach using RANS simulation can be readily applied to estimate the manoeuvrability of WTIV at the initial design stage.*

KEYWORDS: Manoeuvrability; Wind turbine installation vessel (WTIV); OpenFOAM; RANS; Zig-zag; Azimuth; Thrust-vectoring propulsion system.

INDTRODUCTION

Recently, as many are getting interested in renewable energy, especially in wind energy, new orders of Wind Turbine Installation Vessel (WTIV) are increasing, and the size of the WTIV becomes larger and larger. The WTIV is equipped with azimuth pods or thrusters for two main purposes: one for transition from construction yard to the operating field and the other for dynamic positioning prior to unloading of the legs to install the wind turbines. As the WTIV requires large deck space to load as many numbers of the wind turbines as it can carry, the shape of the hull, both bow and stern, is barge type. This barge type vessel is generally difficult to satisfy course keeping ability. To improve its maneuverability, preliminary studies on skeg and increased side projected area of control devices such as pod or azimuth thruster fin, etc. are made at the initial design stage. This study focuses on the manoeuvrability of WTIV estimated by the captive model test such as Planar Motion Mechanism (PMM). Furthermore, numerical studies on this subject are performed in order to check its applicability.

There are a number of different methods to estimate the manoeuvring performance of such vessel at the initial design stage, namely (1) utilization of full scale database, (2) model test, (3) application of empirical method (Kijima and Nakiri, 2003) and (4) numerical approach using Computational Fluid Dynamics (CFD). As mentioned previously, the WTIV is a new type of vessel with uniqueness of hull form, so it is not possible to use the full scale database. Furthermore, it is difficult to apply the

Corresponding author: *Sungwook Lee*, e-mail: *sw8224.lee@samsung.com*

empirical method to the study on improvement in maneuverability with and/or without appendages such as skeg. The rest of two methods are the model test and the numerical approach using CFD, yet again, it is difficult to perform the model test due to high cost in time and expense at the initial design stage. Therefore, it is considered that the estimation of manoeuvring performance using CFD would be the most reasonable and practical method.

Recently, many researchers study and try to verify this computational method so that it is highly expected for the actual application once it is fully developed (Toxopeus, 2011; Simonsen and Stern, 2005; Cura, 2006; Cura et al., 2008; Sakamoto et al., 2012). Over the last decade, the computational method has been successfully applied to estimate ship resistance and self-propulsion performances and now further application to seakeeping and manoeuvring performances (Wilson et al., 2006; Broglia et al., 2013) is being started. Most of these computational studies on seakeeping and manoeuvring performances using CFD are carried out with in-house solvers, and at the same time, there are some on-going studies with the commercial codes. However, the development of studies with the commercial codes is slow because the applicable open-access lines such as KVLCC and KCS from MOERI and DDG destroyer from US Navy are too limited and it is inadequate that there are not many different cases to be applied. Hence, this study presents the computational method to estimate the maneuverability of the WTIV for various reasons as mentioned previously. For present study, OpenFOAM, an open-source CFD toolkit, is used for computation not only because the commercial code does not allow expansion of the work scope but also because it has very powerful potential functionality developed and used by the users researching at the various fields in the world. Moreover, the Planar Motion Mechanism (PMM) function of OpenFOAM, added by Lee et al. (2013) is applied as well. This study starts with introducing the mathematical model with equations of manoeuvring motion of the vessel with thrust vectoring propulsion system. Then the forces and moments applied to the bare hull of WTIV and to the hull with single center skeg and twin skeg are calculated. These calculation results are to be compared with the results of the model test conducted at the model basin. In addition, the manoeuvring hydrodynamic derivatives computed from these forces and moments are used to compare the dynamic stability index and determine whether the course keeping ability has been improved. Finally, the results of zig-zag computational simulation are compared with ones obtained from the captive model test to verify if this computational method is applicable or not.

EQUATION OF MANOEUVRING MOTION AND MATHEMATICAL MODEL

Equation of manoeuvring motion

In general, the equations of ship manoeuvring motion can be expressed by coupling the motions in the horizontal plane i.e surge, sway and yaw. When the coordinate system is defined as Fig. 1, the equations of ship manoeuvring motion can be written as Eq. (1). Here, O-XY is the earth-fixed coordinate system and o-xy is the ship-fixed coordinate system.

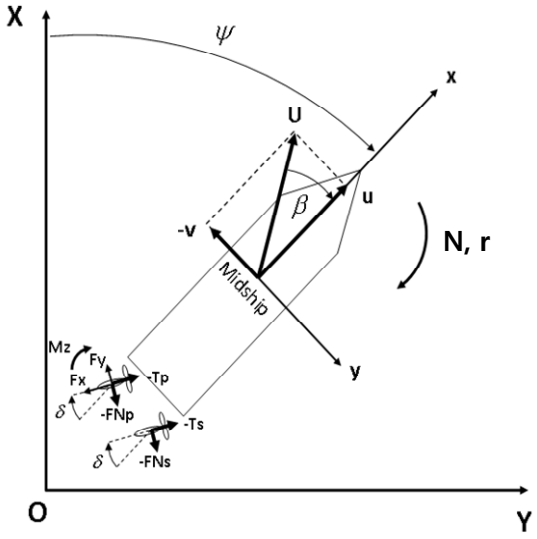

Fig. 1 Coordinate system for describing manoeuvring motion.

$$\begin{aligned} m(\dot{u}-vr-x_G r^2) &= X_H + X_P + X_R \\ m(\dot{v}+ur+x_G\dot{r}) &= Y_H + Y_P + Y_R \\ I_z\dot{r}+mx_G(\dot{v}+ur) &= N_H + N_P + N_R \end{aligned} \tag{1}$$

Here, m is the mass of a ship and I_z is the moment of inertia of a ship in z direction. u, v and r are the longitudinal velocity, transverse velocity and yaw velocity, respectively. x_G is the position of center of gravity forward of mid-ship. The right-hand side terms (*X*, *Y*, *N*) in the Eq. (1) are the external forces(*x* and *y*) and moment(*z*) using manoeuvring motion Mathematical Group (MMG) model. The subscription 'H', 'P' and 'R' in Eq. (1) denotes the hull, propeller and rudder force, respectively. In case of the ship equipped with thrust-vectoring propulsion system, the terms for the propeller and rudder can be replaced by 'TV' term as expressed in Eq. (2) (Yang et al., 2009).

$$\begin{aligned} m(\dot{u}-vr-x_G r^2) &= X_H + X_{TV} \\ m(\dot{v}+ur+x_G\dot{r}) &= Y_H + Y_{TV} \\ I_z\dot{r}+mx_G(\dot{v}+ur) &= N_H + N_{TV} \end{aligned} \tag{2}$$

Here, the subscription '*TV*' means the thrust-vectoring propulsion system. Eqs. (1) and (2) are basically the same equations but with different mathematical model of the external forces for thrust-vectoring. This will be described in further details in the next section.

Mathematical model on hull forces and thrust-vectoring propulsion system

The mathematical model on hull forces which are one component of the external forces can be written as Eq. (3) based on Taylor series:

$$\begin{aligned} X_H &= X_{\dot{u}}\dot{u} + (X_{vr} - Y_{\dot{v}})vr + X_{vv}v^2 + X_{rr}r^2 + X(u) \\ Y_H &= Y_{\dot{v}}\dot{v} + Y_{\dot{r}}\dot{r} + X_{\dot{u}}ur + Y_v v + Y_r r + Y_{vvv}v^3 + Y_{vvr}v^2 r + Y_{vrr}vr^2 + Y_{rrr}r^3 \\ N_H &= N_{\dot{v}}\dot{v} + N_{\dot{r}}\dot{r} + N_v v + N_r r + N_{vvv}v^3 + N_{vvr}v^2 r + N_{vrr}vr^2 + N_{rrr}r^3 \end{aligned} \tag{3}$$

Here, Y_v, Y_r, N_v, N_r ...are the hydrodynamic derivatives and X(u) is the resistance of a ship. Each hydrodynamic derivative can be obtained by the captive model test, the empirical method and numerical method such as RANS calculation. In this study, the hydrodynamic derivatives are obtained by RANS calculation, which is described in the following section.

Meanwhile, the forces due to the thrust-vectoring propulsion system can be calculated by the following Eqs. (4) and (5) as proposed by Yang (2009).

$$\begin{aligned} X_{TV} &= -(1-t)(T_{Sum}\cos\delta - FN_{Sum}\sin\delta) \\ Y_{TV} &= -(1+a_H)(T_{Sum}\sin\delta + FN_{Sum}\cos\delta) \\ N_{TV} &= -(x_{TV}+a_H x_H)(T_{Sum}\sin\delta + FN_{Sum}\cos\delta) \end{aligned} \tag{4}$$

$$\begin{aligned} T_{Sum} &= T_{Port} + T_{Stbd} \\ FN_{Sum} &= FN_{Port} + FN_{Stbd} \end{aligned} \tag{5}$$

Here, x_{TV} in Eq. (4) represents a distance between the mid-ship and the position of the each thrust-vectoring propulsion system and others such as a_H, x_H are the interaction coefficients between the hull and propulsion units. In addition, 'T' and 'FN' in Eq.

(5) represent thrust and normal force of the thrust-vectoring propulsion system, respectively. Although thrust T in Eqs. (4) and (5) is a function of propeller advance coefficient J and steering angle of the thrust-vectoring propulsion system δ according to Yang et al. (2009), it is assumed that thrust T is only a function of K_T in this study.

$$T = \rho n^2 D^4 K_T(J)$$
$$FN = \frac{1}{2}\rho U_R{}^2 A_R f_\alpha \sin\alpha_R \tag{6}$$

The detailed information about all variables in Eq. (6) can be found in Yang et al. (2009) and Kijima and Nakiri (2003).

MODEL TEST

In order to check the accuracy of RANS calculation, the captive model tests (especially, PMM) of the bare hull and the hull with twin skeg were carried out. The principal dimensions and the general arrangement of WTIV are presented in Table 1 and Fig. 2, respectively. As shown in Table 1 and Fig. 2, WTIV has the wide breadth and barge-type stern hull form.

Table 1 Principal dimensions of WTIV.

Particulars	Draught conditions	
	Full scale design	Model scale design
Length between perpendiculars	155.6 *m*	7.521 *m*
Breadth, moulded	49.0 *m*	2.368 *m*
Draught at FP	5.5 *m*	0.266 *m*
Draught at AP	5.5 *m*	0.266 *m*
C_B	0.8	0.8

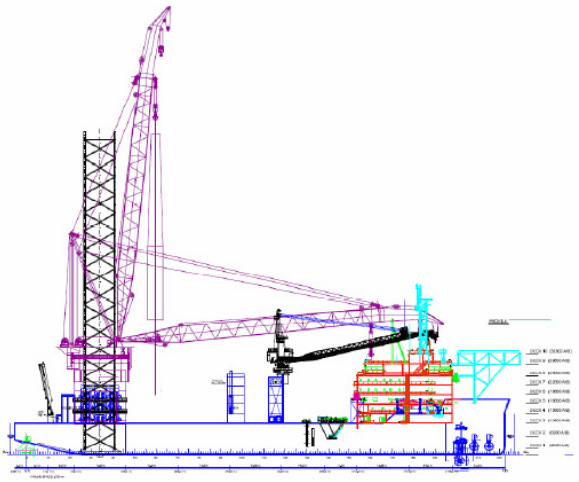

Fig. 2 General arrangement of WTIV.

The following Fig. 3 shows the model used in the captive model test. In order to check the effect of the skeg for the course keeping ability, the captive model tests were carried out for both cases, with and without twin skeg.

Fig. 3 Model ship of WTIV.

Figs. 4 and 5 compare the lateral force and yaw moment in both cases, respectively. As shown in Fig. 4, the lateral force acting on the hull with skeg is larger than that on the bare hull and the yaw moment acting on the hull with skeg is smaller than that on the bare hull. This means that the skeg behaves as the additional lateral projected area for the hull and contributes to decrease in the yaw moment which causes rotation of the hull. It can be thought that the hull with skeg is relatively better than the bare hull in course keeping ability.

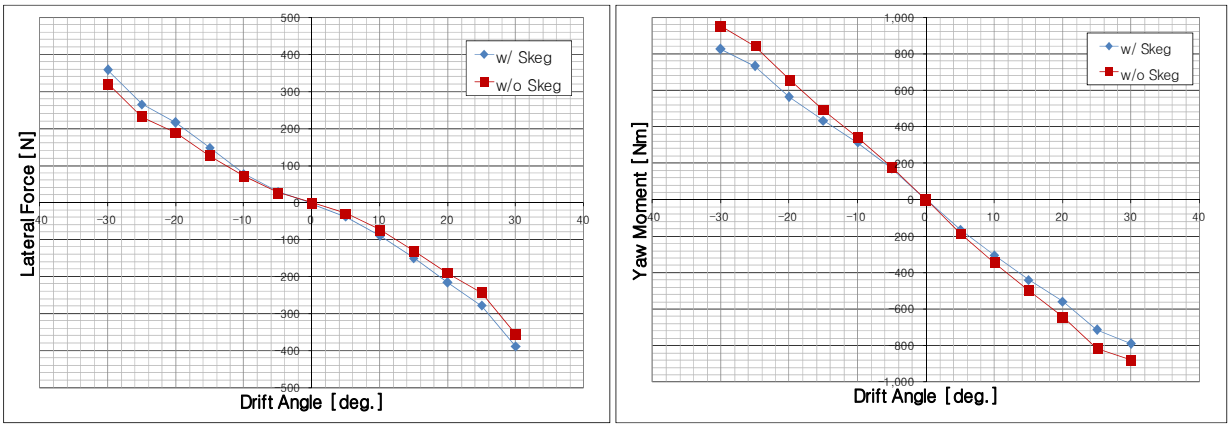

Fig. 4 Lateral force and yaw moment in static drift for w/o skeg and w/ twin skeg.

In order to evaluate the course keeping ability, the dynamic stability index (=L_r'-L_v') is investigated and the results are summarized in Table 2. Here, L_v'(=N_v'/Y_v') is a moment arm, the ratio of the yaw moment to the lateral force due to the lateral motion while L_r'(=(N_r'-$x_G m'$)/(Y_r'-m')) is a moment arm, the ratio of the yaw moment to the lateral force due to the yaw motion. It should be noted that all the values in Table 2 are obtained from the least square fitting. The linear fittings for the hydrodynamic derivatives due to the pure yaw motion are shown in Fig. 5. According to Figs. 4 and 5, when the twin skeg is applied to the bare hull, increase in the side projected area at the stern of the hull makes the lateral force due to the lateral motion become larger, and the yaw moment due to the lateral motion become smaller. This observation is found in case of the yaw motion as well. This mechanism can also be explained by the dynamic stability index in more detailed manner.

Table 2 Comparison results for the dynamic stability index (w/o skeg and w/ twin skeg).

Config.	Y_v'	N_v'	Y_r'-m'	N_r'-$x_G m'$	L_v'	L_r'	L_r'-L_v'
w/o Skeg	-0.1517	-0.1276	-0.5302	-0.00724	0.84113	0.0135	-0.8267
w/ Skeg	-0.1887	-0.1139	-0.5096	-0.01193	0.60360	0.0234	-0.5802

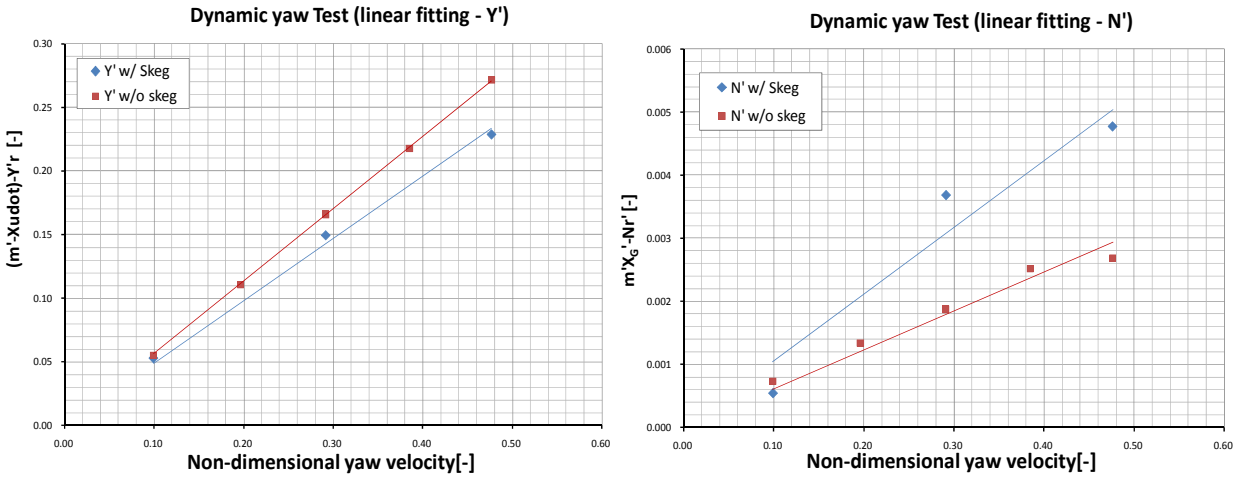

Fig. 5 Hydrodynamic derivatives due to pure yaw motion for w/o skeg and w/ twin skeg.

In general, when the dynamic stability index (=L_r'-L_v') becomes positive value (>0), the course keeping ability is stable. In other words, when the dynamic stability index is negative (<0) the course keeping ability becomes unstable. From all the experimental results, the dynamic stability indices are negative for both cases i.e. without skeg and with twin skeg. This means that the course keeping ability of both cases is unstable. However, the course keeping ability of the hull with twin skeg is relatively stable than the bare hull case as the index is closer to zero value.

NUMERICAL CALCULATIONS USING RANS (OpenFOAM)

As mentioned previously, (U)RANS calculations were carried out to obtain the manoeuvring hydrodynamic derivatives. In this study, especially, OpenFOAM was used as a (U)RANS solver. OpenFOAM is an open-source CFD toolkit based on the finite volume method with unstructured grids. OpenFOAM has been used in various fields for many different applications. For more detailed information about applications of OpenFOAM, reference is made to Jasak and Henrik (2009). No free-surface effect is considered in the (U)RANS calculation of the present study and the PMM functionality which has been implemented in Lee et al. (2013) was used in the static drift and pure yaw cases. The grid system used for OpenFOAM calculation is shown in Fig. 6.

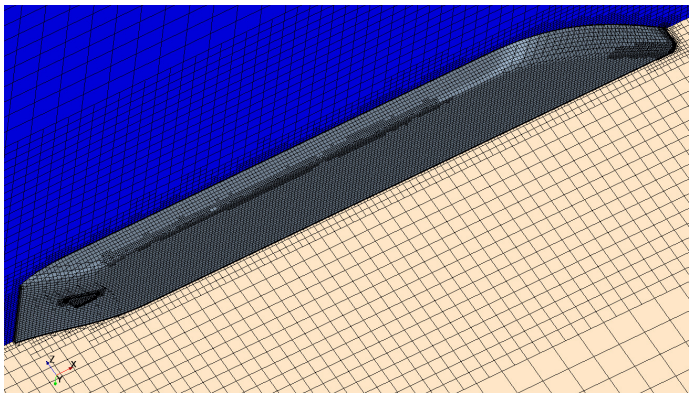

Fig. 6 Example of the grid system for OpenFOAM calculation.

Total grid size used for both cases of the static drift and the pure yaw is about 0.35 M cells. Standard k-ε was selected for the turbulence model, and wall function was used with Y^+<100 for all calculations made in this study. Furthermore, some additional calculations of the static drift cases were carried with commercial code of ANSYS Fluent. The reason for Fluent computation is to compare the level of other RANS computation to OpenFOAM computation since the calculation result of yaw moment at large drift angle from OpenFOAM come out to be smaller than the model test results, as shown in Fig. 7.

Fig. 7 compares the results of lateral force for the static drift case between the model test and the (U)RANS calculation. As shown in Fig. 7, both CFD calculations of OpenFOAM and ANSYS Fluent overpredict the lateral force in its magnitude while they underpredict the yaw moment compared to the model test values. As shown in Fig. 7, the differences between the results of the RANS calculations and the experiment are observed at large drift angle for both of the lateral force and the yaw moment. It can be thought as that these differences are mainly due to the turbulence model, grids and the effect of free-surface. Although the difference is observed at large drift angle, it is meaningful in terms of the linear hydrodynamic derivatives. Therefore, the further study on this subject is not carried out in the present study.

As the time history of the lateral forces in pure yaw motion (r'=0.3) obtained from RANS calculation based on OpenFOAM and model test results are compared, they are well matched to each other as shown in Fig. 8.

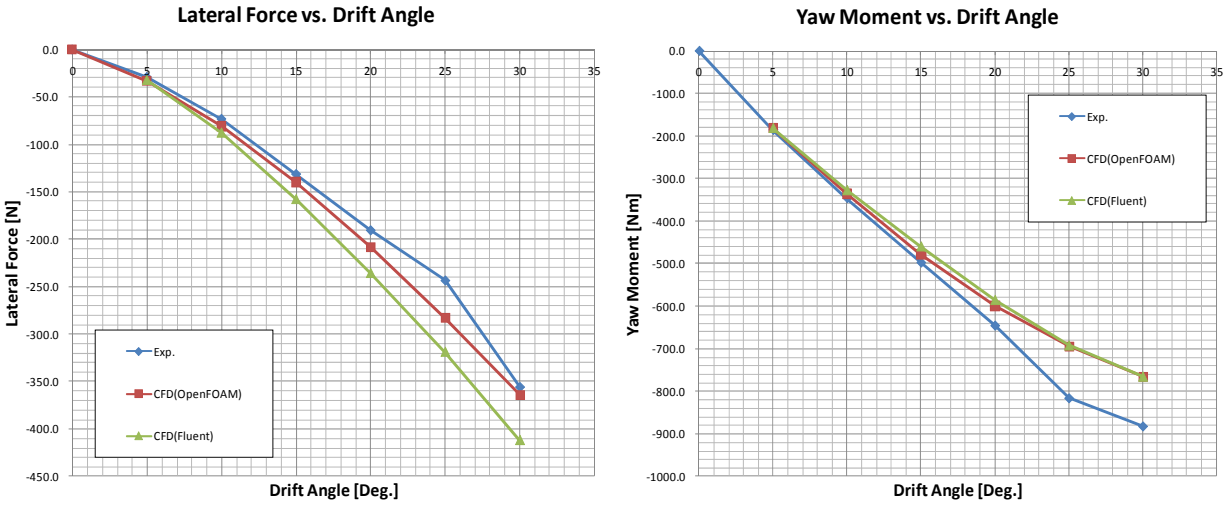

Fig. 7 Lateral force and yaw moment in static drift
(comparisons between experiment and RANS calculations for bare hull).

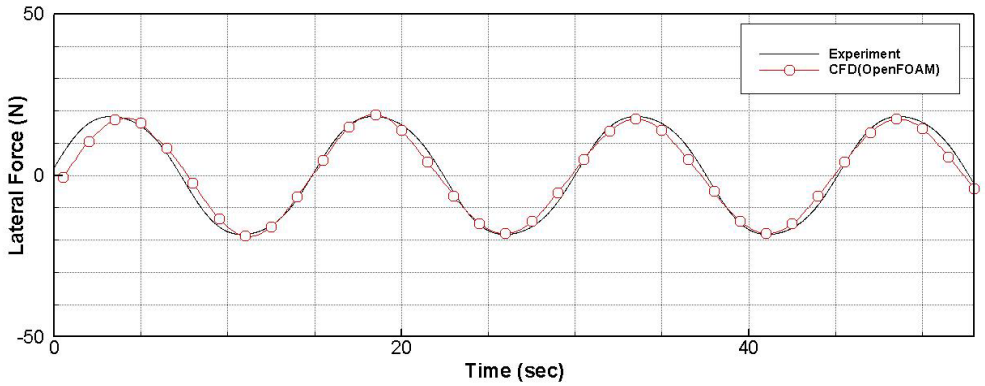

Fig. 8 Lateral force in pure yaw motion (comparison between experiment and RANS calculation for r'=0.3).

Also, the linear hydrodynamic derivatives are compared as shown in Table 3. The differences in the linear hydrodynamic derivatives of the lateral force due to the lateral motion and of the yaw moment due to the yaw motion are 18% and 25%, respectively. 25% error of the yaw moment due to the yaw motion seems large but it is a reasonable level as the experimental result N_r' (yaw moment due to yaw motion) is small except the Y_v', it can be thought that other linear hydrodynamic derivatives agree well with the model test. For the accuracy of the Y_v', it seems that the studies such as the grid sensitivity, calculation time step and turbulence model are necessary to be carried out. The differences can be minimized after study on the effect of these parameters is carried out.

In order to investigate the effect of the skeg in the course keeping ability, the configurations of the skeg shown in Table 4

and Fig. 3 are considered and the calculation for each configuration of the skeg is carried out. The numerical results obtained from the both static drift and pure yaw calculations are shown in Figs. 9 to 11.

Table 3 Comparison results for the linear hydrodynamic derivatives (experiment and RANS calculation).

	Y_v'	N_v'	Y_r'-m'	N_r'-x_G'm'
Exp.	-0.151734	-0.127573	-0.5302	-0.00724
CFD(OpenFOAM)	-0.178931	-0.126589	-0.5310	-0.00540
Error((CFD-Exp.)/Exp.)	+18%	-0.8%	0.2%	+25%

Table 4 Configurations of skeg.

	Lateral projected rudder area[m^2]	Remark[-]
Center skeg	19.314	Original
Twin skeg1	9.657	50% of original
Twin skeg2	13.781	70% of original

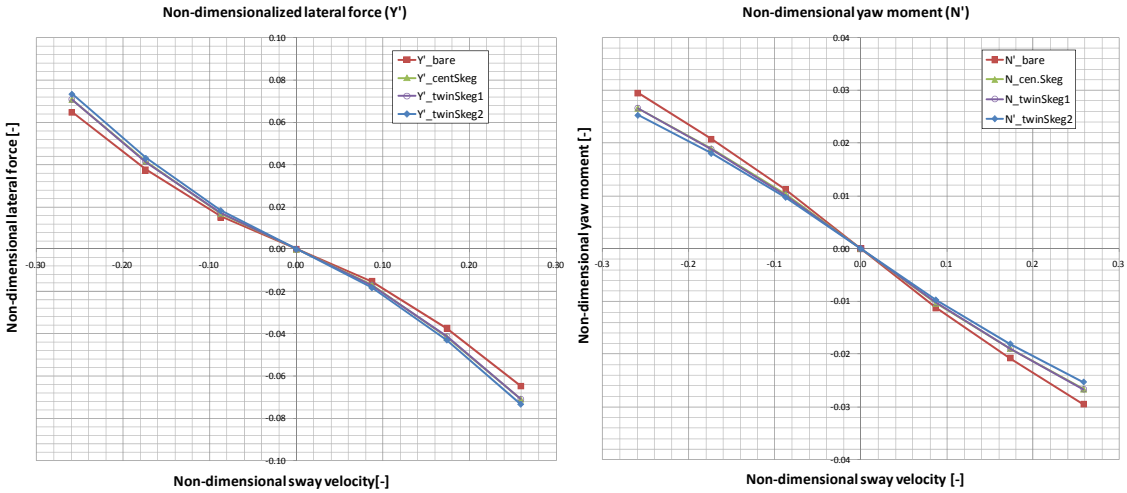

Fig. 9 Non-dimensional lateral force and yaw moment in static drift (comparisons between w/o skeg and w/ skeg, RANS calculations).

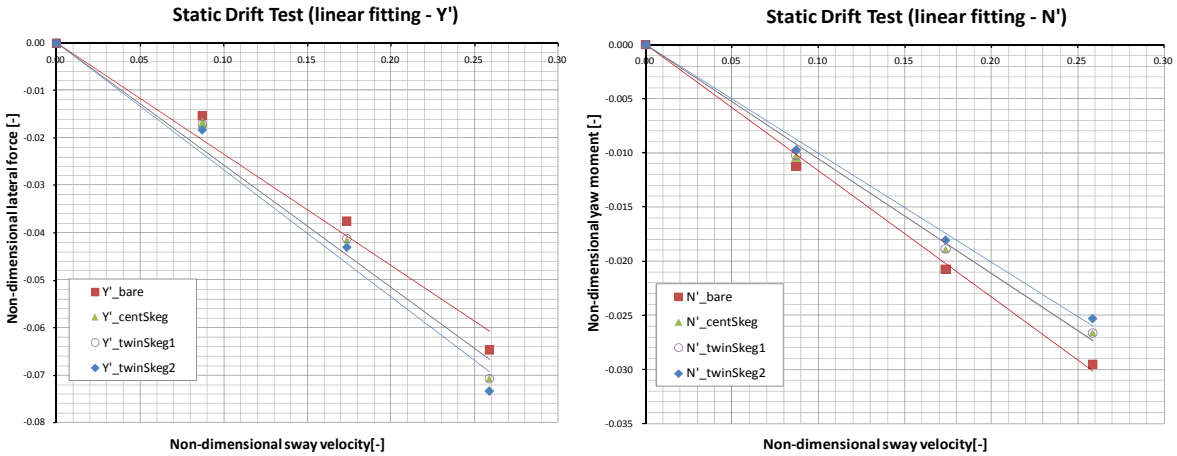

Fig. 10 Hydrodynamic derivatives due to pure sway motion (comparisons between w/o skeg and w/ skeg, RANS calculations).

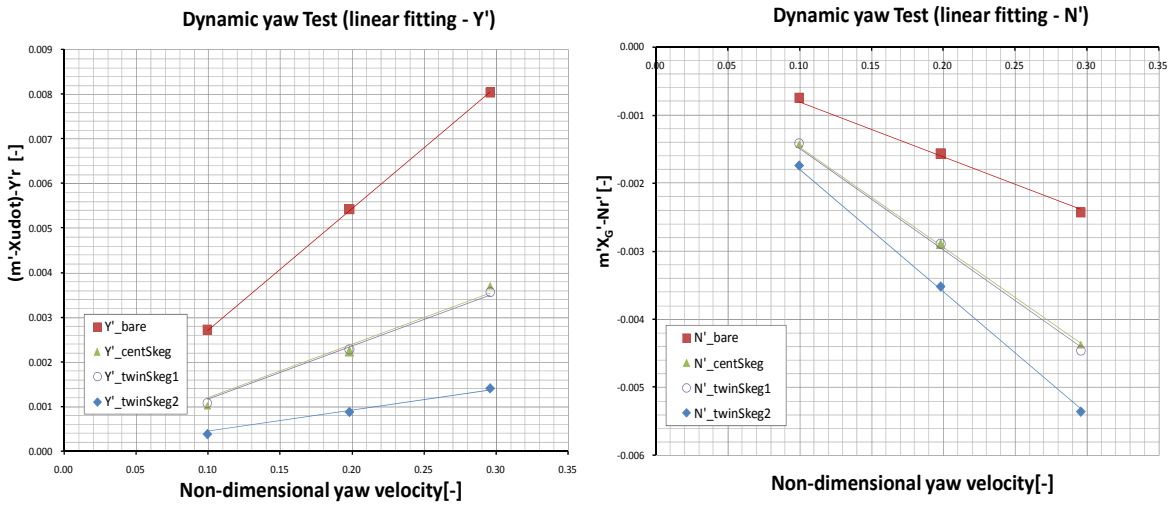

Fig. 11 Hydrodynamic derivatives due to pure yaw motion
(comparisons between w/o skeg and w/ skeg, RANS calculations).

As shown in Figs. 9 to 11, the forces and moment acting on the hull with the skeg make the hull more stable in the course keeping ability than those on the hull without the skeg(refer to Table 2 showing that the dynamic stability index becomes stable)**.** Especially, when the twin skeg has the same lateral projected area as the single center skeg where the area of one side of the twin skeg is 50% of single skeg area, the same course keeping ability as the single center skeg is observed. Of course, the course stability will depend on the location of the twin skeg on the hull. However, it still shows that the twin skeg with the same lateral projected area with the single center skeg can obtain the same course keeping ability. However, it is thought that these results are limited to the configuration presented in this study only so that further study on this subject is necessary. The contour of the pressure distribution acting on the stern in drift angle of 15° are shown in Fig. 12. It is observed that the positive pressure distribution on the stern part of the hull with twin skeg is wider than that on the hull with center skeg. With wider positive pressure distribution, the yaw moment due to the lateral motion is reduced, and consequently, the dynamic stability becomes more stable.

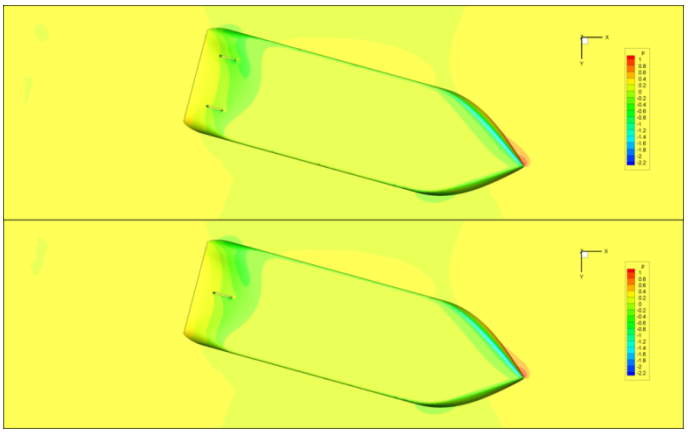

Fig. 12 Contour of the pressure distribution acting on the hull in static drift case (drift angle=15°).

The observed trend of the dynamic stability index according to the effect of the skeg is summarized in Table 5. Although there are quantitative discrepancies between CFD and EFD results as shown in Table 5, the effect of the skeg is clearly observed in a qualitative manner. From this, it is concluded that improvement of maneuverability with and without the skeg can be predicted through CFD. From Table 5, it can be thought that the hull with the twin skeg which has 70% lateral projected area of the single center skeg in one side is most stable in the course keeping ability.

Table 5 Comparison results for the dynamic stability index (EFD and CFD).

	EFD		CFD				CFD/EFD	
	w/o skeg	w/ twin skeg2	w/o skeg	w/ center skeg	w/ twin skeg1	w/ twin skeg2	w/o skeg	w/ twin skeg2
Yr'-m'	-0.5302	-0.5096	-0.5310	-0.5137	-0.5145	-0.5075	100.2%	99.6%
Nr'-xG'm'	-0.0072	-0.01193	-0.0054	-0.0122	-0.0120	-0.0153	75.2%	128.0%
Ir'	0.0135	0.02341	0.01017	0.02377	0.02336	0.03008	75.1%	128.5%
Yv'	-0.1517	-0.1887	-0.1789	-0.1992	-0.1992	-0.2110	117.9%	111.8%
Nv'	-0.1275	-0.1139	-0.1266	-0.1170	-0.1158	-0.1108	99.3%	97.3%
Iv'	0.8403	0.604	0.7075	0.5873	0.5813	0.5252	84.2%	87.0%
Stability lever	-0.8267	-0.5802	-0.697	-0.564	-0.558	-0.495	84.3%	85.3%

NUMERICAL SIMULATIONS FOR ZIG-ZAGMANOEUVRINGMOTION

In order to predict zig-zag manoeuvring motion which is one of IMO manoeuvring criteria, the numerical simulation was carried out by using Eq. (2) and the hydrodynamic derivatives obtained from both the RANS calculation and the model test. Figs. 13 and 14 compare the results of the zig-zag motion the RANS calculations and model test for bare hull and hull with twin skeg, respectively. These comparisons show that the zig-zag motions from the RANS calculations are in good agreement with the model test results.

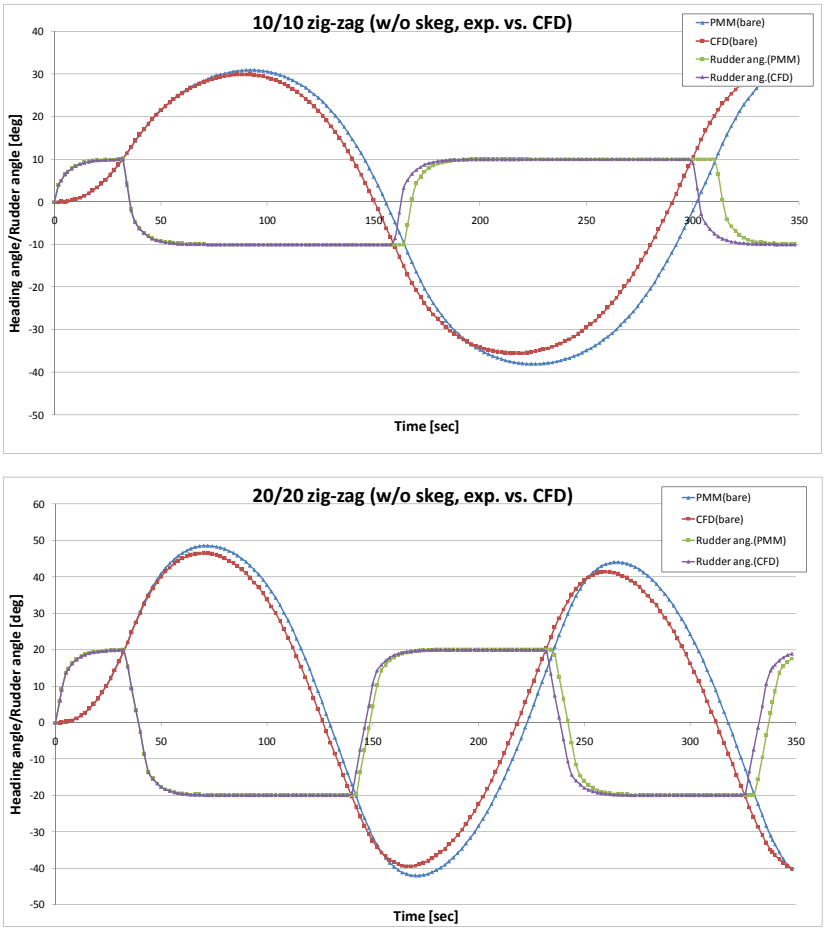

Fig. 13 Comparison of the zig-zag calculations without the skeg (EFD vs. CFD).

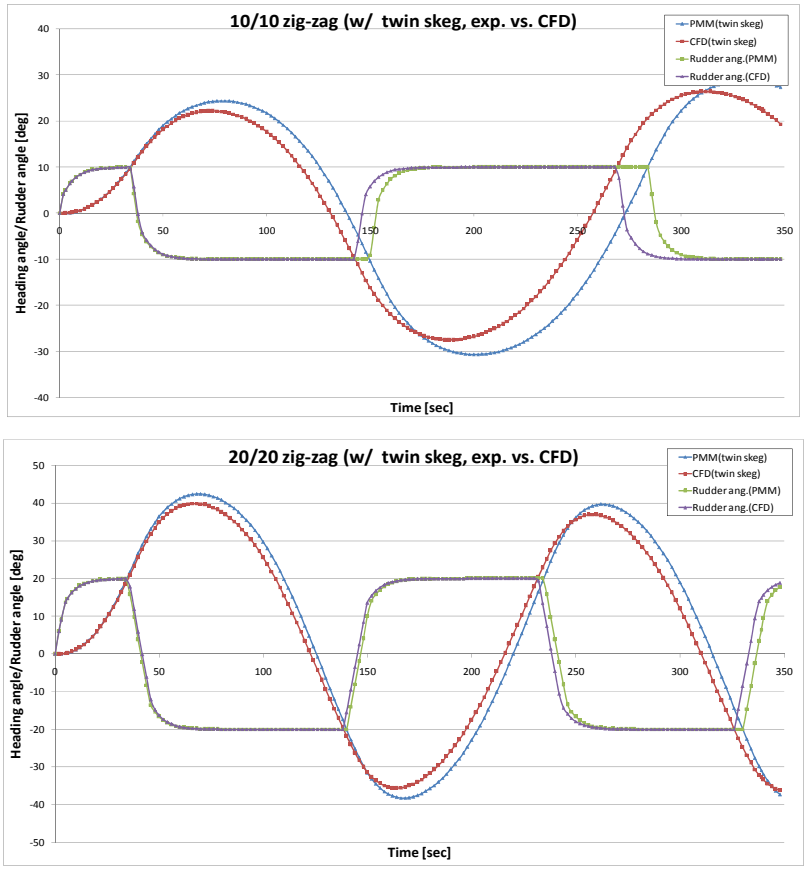

Fig. 14 Comparison of the zig-zag calculations with the twin skeg (EFD vs. CFD).

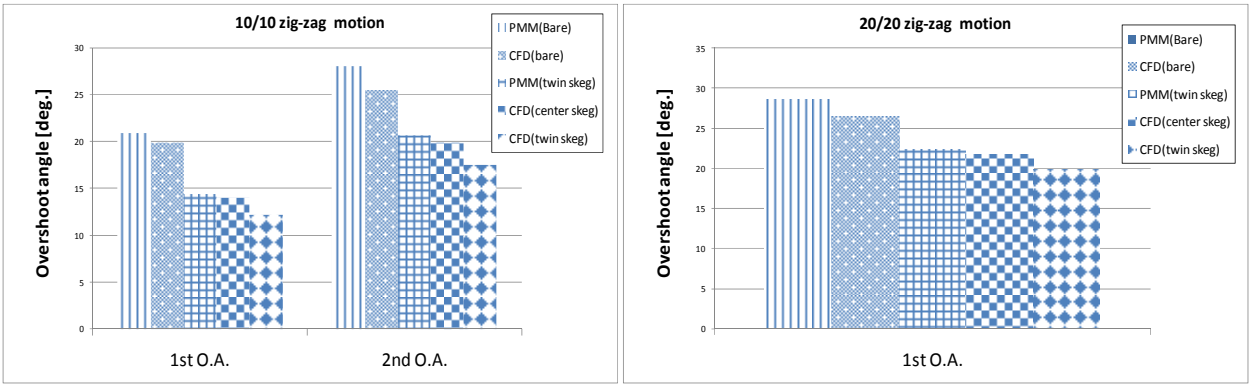

Fig. 15 Comparison results of the overshoot angles in 10/10 and 20/20 zig-zag motion (EFD vs. CFD).

Table 6 Comparison results for the zig-zag motions (EFD vs. CFD).

	EFD		CFD			Error	Error
	PMM (Bare)	PMM (twin skeg2)	CFD (bare)	CFD (center skeg)	CFD (twin skeg2)	Bare	Twin skeg2
10/10 zig-zag							
1st O.A.	20.9	14.4	19.9	14	12.2	-5%	-15%
2nd O.A.	28	20.7	25.5	19.9	17.5	-9%	-15%
20/20 zig-zag							
1st O.A.	28.6	22.4	26.5	21.7	19.9	-7%	-11%

More detailed information can be found in Fig. 15 and Table 6. Compared to the model test results, the CFD calculation results for the bare hull case and the twin skeg case differ by maximum of -9% and -15%, respectively. These discrepancies may be resulted from the different hydrodynamic derivatives obtained from the model tests and RANS calculations. As discussed previously, the zig-zag calculations are consistent with the results observed in the analysis of the dynamic stability index. Hence, it is evident that the RANS calculations can offer quite useful information in prediction of the manoeuvrability for variations in the shapes of both appendage and stern hull form, to a designer at the initial design stage from practical perspective. Although there is a lack of accuracy in the results, more accurate results are expected to be achieved through more extensive studies such as the grid sensitivity, various schemes, and the turbulence model.

CONCLUSIONS

This study presented a number of topics. One was the manoeuvrability of Wind Turbine Installation Vessel (WTIV) with thrust-vectoring propulsion system through the PMM model test. In addition to the model test, the numerical study is also performed in order to investigate the maneuverability of the WTIV, with thrust-vectoring propulsion system. The RANS calculation which can be used to estimate the manoeuvrability of the WTIV with thrust-vectoring propulsion system was carried out at the initial design stage. Throughout this study, the proposed method is quite effective when the maneuverability of a vessel is needed to be evaluated at the initial design stage prior to any model tests. For this purpose, it was shown that the proposed approach is well worth using in understanding the change of the maneuverability depending on the various configuration of the appendage. In addition, it is shown that the twin skeg with 50% of the lateral project area of the single center skeg can give the same effect in the course keeping ability from the numerical calculation. But further studies are necessary to confirm whether the same results can be obtained. Furthermore, an extensive sensitivity studies about, such as, grid system, turbulence model and scheme, should be carried out in near future to achieve higher accuracy of the RANS calculations.

REFERENCES

Broglia, R., Dubbioso, G., Durante, D. andMascio, A.D., 2013. Simulation of turning circle by CFD: Analysis of different propeller models and their effect on manoeuvring prediction. *Applied Ocean Research*, 39, pp.1-10.

Cura, H.A., 2006. Virtual PMM tests for manoeuvring prediction. *In 26th Symposium on Naval Hydrodynamics*, Rome, Italy, 2006, pp.31-49.

Cura, H.A., Vogt, M. and Gatchell, S., 2008. Manoeuvring prediction for two tankers based on RANS simulations. *In SIMMAN Workshop on Verification and Validation of Ship Manoeuvring Simulation Methods*, Copenhagen, Denmark, 2008, pp.23-28.

Jasak, H. and Henrik, R., 2009. Dynamic mesh handling in OpenFoam. *Proceeding of the 47th Aerospace Sciences Meeting Including The New Horizons Forum and Aerospace Exposition*, Orlando, Florida, 2009.

Kijima, K. and Nakiri, Y., 2003. On the practical prediction method for ship manoeuvring characteristics. *Transaction of the West Japan Society of Naval Architects*, 105, pp.21-31.

Lee, S.W., Kwon, S.C., Lee, D. and Seo, J., 2013. Study on manoeuvring hydrodynamic forces using open-source CFD toolkit (OpenFOAM). *Proceedings of the Eighth International Workshop on Ship Hydrodynamics*. Seoul, 24 October 2013.

Sakamoto, N., Carrica, P.M. and Stern, F., 2012. URANS simulations of static and dynamic manoeuvring for surface combatant: part 1. Verification and validation for forces, moment, and hydrodynamic derivatives. *Journal of Marine Science and Technology*, 17(4), pp.422-445.

Simonsen, C.D. and Stern, F., 2005. RANS manoeuvring simulation of Esso Osaka with rudder and a body-force propeller. *Journal of Ship Research*, 49(2), pp.98-120.

Toxopeus, S.L., 2011. *Practical application of viscous-flow calculations for the simulation of manoeuvring ships*. PhD. thesis, TU Delft, Delft University of Technology.

Wilson, R.V., Carrica, P.M. and Stern, F., 2006. Unsteady RANS method for ship motions with application to roll for a surface combatant. *Computers & fluids*, 35(5), pp.501-524.

Yang, H., Kwon, C., Lee, Y. and Park,G., 2009. Prediction of the manoeuvrability on twin poded vessel. *Proceedings of Marine Simulation and Ship Manoeuvrability 2009(MARSIM09)*, Panama city, Panama, 2009.